Colloids and Surfaces B: Biointerfaces 163 (2018) 385–393

Contents lists available at ScienceDirect

Colloids and Surfaces B: Biointerfaces

journal homepage: www.elsevier.com/locate/colsurfb

Rapid *in situ* biosynthesis of gold nanoparticles in living platelets for multimodal biomedical imaging

Juan Jin [1], Taotao Liu [1], Mingxi Li, Chuxiao Yuan, Yang Liu, Jian Tang, Zhenqiang Feng, Yue Zhou, Fang Yang*, Ning Gu*

State Key Laboratory of Bioelectronics, Jiangsu Key Laboratory for Biomaterials and Devices, School of Biological Sciences and Medical Engineering, Southeast University, Sipailou 2, Nanjing, Jiangsu, 210009, PR China

ARTICLE INFO

Article history:
Received 27 September 2017
Received in revised form
14 December 2017
Accepted 9 January 2018
Available online 10 January 2018

Keywords:
Gold nanoparticles
Platelets
Ultrasound
In situ biosynthesis
Imaging

ABSTRACT

Inspired by the nature, the biomimetic nanomaterial design strategies have attracted great interest because the bioinspired nanoplatforms may enhance the functionality of current nanoparticles. Especially, the cell membrane-derived nanoparticles can more effectively navigate and interact with the complex biological microenvironment. In this study, we have explored a novel strategy to rapidly *in situ* biosynthesize gold nanoparticles (GNPs) in living platelets with the help of ultrasound energy. Firstly, under the ultrasound exposure, the biocompatible chloroauric acid salts ($HAuCl_4$) can be enhanced to permeate into the platelet cytoplasm. Then, by the assist of reducing agent ($NaBH_4$ and sodium citrate) and platelet enzyme, GNPs were fast *in situ* synthesized in intra-platelets. The biosynthesized GNPs had a size of about 5 nm and were uniformly distributed in the cytoplasm. Atomic absorption spectrometry (AAS) showed the synthesized amount of Au is $(12.7 \pm 2.4) \times 10^{-3}$ pg per one platelet. The GNPs in platelets can produce Raman enhancement effect and further be probed for both dark-field microscopy (DFM)-based imaging and computed tomography (CT) imaging. Moreover, the platelets were not activated and remained aggregation bioactivity when intra-platelet GNPs synthesis. Therefore, such mimicking GNPs-platelets with *in situ* GNPs components remain inherent platelet bioactivity will find potential theranostic implications with unique GNPs properties.

1. Introduction

Nanomaterials have been designed to provide a platform to integrate diagnosis and therapy in biomedical applications because of their unique performance [1–4]. Due to many excellent properties such as nano size, surface modification, a high scattering cross section and resistance to photobleaching, gold nanoparticles (GNPs) are widely used for bioimaging, biosensing, as well as photothermal therapy [5–8]. However, it is found that, a wide range of interesting characteristics of GNPs are size- and/or shape-related [9]. Therefore, many chemical preparation methods have been developed to well control the GNPs' different sizes and shapes. Tapan K. Sau et al. utilized seed-mediated growth methods to produce various morphology and dimensions of Au nanocrystals [10]. Xiaohui Ji et al. reported the synthesis of gold nanocrystals with different size by using citrate reduction method [11].

However, for *in vivo* applications, the naked GNPs can be readily recognized by the immune system, removed from circulation, and stored in the liver and kidneys [12,13]. In order to achieve their *in vivo* effectiveness and targeting manipulation in complex physiological microenvironment, many surface modification and/or complex fabrication strategies have been developed. Especially, biological agents including plant tissues, bacteria, fungi, etc. [14–16] are used to synthesize and modify the surface of GNPs by providing with natural capping [17]. Besides, utilizing special microenvironment of tumor cells, gold nanoclusters had been biosynthesized *in situ* in tumor cells to escape the clear of immune system. Xuemei Wang et al. reported *in vivo* self-bio-imaging of tumors through *in situ* biosynthesized gold nanoclusters [12,18]. These biosynthesized GNPs have many advantages including nontoxic green chemistry procedures and high cost-effectiveness [19], which can -engineer GNPs with desired capping to play a role in specific application such as bio-labeling and cancer therapy [20,21]. However, there is no report on *in situ* biosynthesis of GNPs in normal cells.

* Corresponding authors.
E-mail addresses: yangfang2080@seu.edu.cn (F. Yang), guning@seu.edu.cn (N. Gu).
[1] These authors contributed equally.

https://doi.org/10.1016/j.colsurfb.2018.01.009
0927-7765/

With the development of biology and biotechnology, cells including erythrocytes, leukocytes and stem cells are novel drug carriers that can be engineered as Trojan horse for drug delivery and cell-based therapy [22,23]. Nanomaterial-loaded engineered cells are promising theranostic platform due to the natural cell bioactivity. Platelets act as sentinels of circulatory system and perform many functions such as hemostasis and the repair of endothelium [24]. Produced by megakaryocytes, platelets have no cell nucleus but contain organelles needed for protein synthesis [25]. A unique set of surface natural moieties endow platelets multiple characteristics including immune evasion, sub-endothelium adhesion, and pathogen interactions [26]. Thus, the platelets have become natures long-circulating delivery vehicles and have inspired the design of many platelet-based functional nanocarriers [27–30]. Hu et al. reported the preparation of nanoparticles enclosed in platelets membrane by adopting a cell membrane cloaking technique [31], which reduces the uptake by macrophage-like cell and enhances the therapeutic efficacy when delivering drugs. However, these membrane cloaking techniques remain some disadvantages. For example, the enclosed nanoparticles should be pre-prepared through a complicated process and the platelet membrane derived by a repeated freeze-thaw process would lose or affect the inherent bioactivity of cell. Moreover, it may exist low cloaking efficiency during cloaking with nanoparticles [32].

Here, we first explored a novel strategy to rapidly *in situ* biosynthesize GNPs in living platelets with ultrasound assistance. With this method, sufficient amount of GNPs in platelets can be obtained (about 30 min) without complex procedures and rigorous conditions. Firstly, platelets were mixed with both chloroauric acid and reducing agent. Assisted by ultrasound exposure and platelet intracellular enzyme, GNPs can be synthesized in the inner side of platelets. Rapid synthesis of GNPs under mild conditions makes it possible to maintain natural characteristics of the living platelets. The presence of GNPs in platelets has been confirmed by UV–vis absorption spectrum, atomic absorption spectrometry (AAS), energy dispersive X-ray spectroscopy (EDS) and transmission electron microscope (TEM). The effects of platelets on morphology, protein components and aggregation performance were investigated by scanning electron microscope (SEM), flow cytometry, protein electrophoresis and spectrophotometric method respectively. Such Trojan horse-like platelets with *in situ* intracellular GNPs components remained natural platelets' bioactivity, as well as their biomedical applications for surface enhanced Raman scattering (SERS) [33], computed tomography (CT) [34] and dark field microscopy-based optical imaging [35] due to the existence of unique GNPs properties.

2. Experimental

2.1. Materials and instruments

Chloroauric acid ($HAuCl_4$), sodium citrate and sodium borohydride ($NaBH_4$) were purchased from Sigma Aldrich, USA. Unexpired (in-dated) human type O-platelet rich plasma (PRP) in acid-citrate-dextrose (ACD) was obtained from Zhongda hospital affiliated to Southeast University. Milli-Q water was used throughout the experiment. Ultrasound exposure was provided by an ultrasonicator (DM200, Shenzhen DIMIP Technology Co., Ltd., China).

2.2. Biosynthesis of gold nanoparticles in platelets

PRP was centrifuged at 3000 r/min for 5 min at room temperature to remove plasma fraction. Platelets were resuspended in equivalent volume of 0.9% sodium chloride solution. GNPs were prepared by $NaBH_4$ reduction of $HAuCl_4$ in the presence of sodium citrate. $HAuCl_4$ was added into platelet suspension at concentration of 24.28 mM. Samples were divided into two groups: one group was subjected to ultrasonic treatment for 60 s using the ultrasonicator (1.00 MHz, 0.25 W/cm^2) with pulse wave at pulse duration time of 1 ms, which is defined as US-GNPs-PLTs group; Another group was without ultrasound exposure, which is defined as GNPs-PLTs group. Then both the platelets suspensions were mixed with sodium citrate and fresh sodium borohydride at concentration of 10 mM and 5 mM respectively. The mixtures were incubated with shaking at 37 °C for 30 min. After reaction, platelets were separated from GNPs in solution by centrifugation at 3000 r/min for 5 min. After 5 times repeated washes, platelets were suspended in saline to obtain the GNPs loaded platelets.

2.3. Characterization of gold particles in platelets

The size distribution of engineered platelets was analyzed by using a 90Plus Particle Size Analyzer (Brookhaven Instrument Corporation). Platelets loading GNPs were lysed with hydrochloric acid and characterized through UV–vis spectroscopy using a UV-3600 spectrophotometer (Shimadzu, Japan). The weight content of GNPs synthesized in platelets was determined by using anatomic absorption spectrometer (model 180-80, Hitachi, Japan). The morphology of platelet was studied with a scanning electron microscope (SEM, FEISirion-200, USA) working under acceleration voltage of 1.00 kV. An energy-dispersive X-ray spectroscope (EDS) attached to the SEM was used to analyze the platelets composition. The intracellular distribution of GNPs in platelets was studied by transmission electron microscope (TEM) as follows. Platelets were first fixed by 2.5% glutaraldehyde at room temperature for half an hour, and subsequently embedded in epon (Sigma-Aldrich, MO, USA). Then the sample was ultrathin sectioned and stained with 1 wt% uranyl acetate before imaging by TEM (JEOL, JEM-2000EX, Japan).

2.4. Side scattering measurement by flow cytometry

Side scattering measurement can be used to analyse the cellular nanoparticle. After synthesis of GNPs, platelets were collected and washed 5 times. The cell pellet was resuspended in 0.9% sodium chloride solution and analyzed by flow cytometry (BD, USA) by measuring the side scatting intensity (SSC). At least 10000 cells were analyzed for each treatment. Results were analysised using software FlowJo 7.6.

2.5. Platelet aggregation assay

Aggregation of platelets was assessed using a spectrophotometric method as reported [31]. PLTs, GNPs-PLTs and US-GNPs-PLTs were resuspended in 0.9% sodium chloride solution (1 mL) and transferred into 24-well plates. 500 μL of human thrombin (Sigma Aldrich, USA) at concentration of 100 IU/mL was added into the suspensions. Absorbance at 650 nm was immediately recorded by TeCan Infinite M200 reader over time. Platelet aggregation was observed based on the reduction of turbidity. Each sample was assayed in replicate (n = 3).

2.6. SDS-PAGE electrophoresis

PLTs were lysed by cell lysis buffer for Western and IP (Beyotime Biotechnology, Haimen, China) with equal volume. Then they were normalized to equivalent overall protein concentration using a SDS-PAGE Assay Kit (Beyotime Biotechnology, Haimen, China). Identification of key membrane proteins by SDS-PAGE electrophoresis with 10% separation gel and 5% spacer gel (Beijing Liuyi Instrument Factory, China). The completed gel was stained

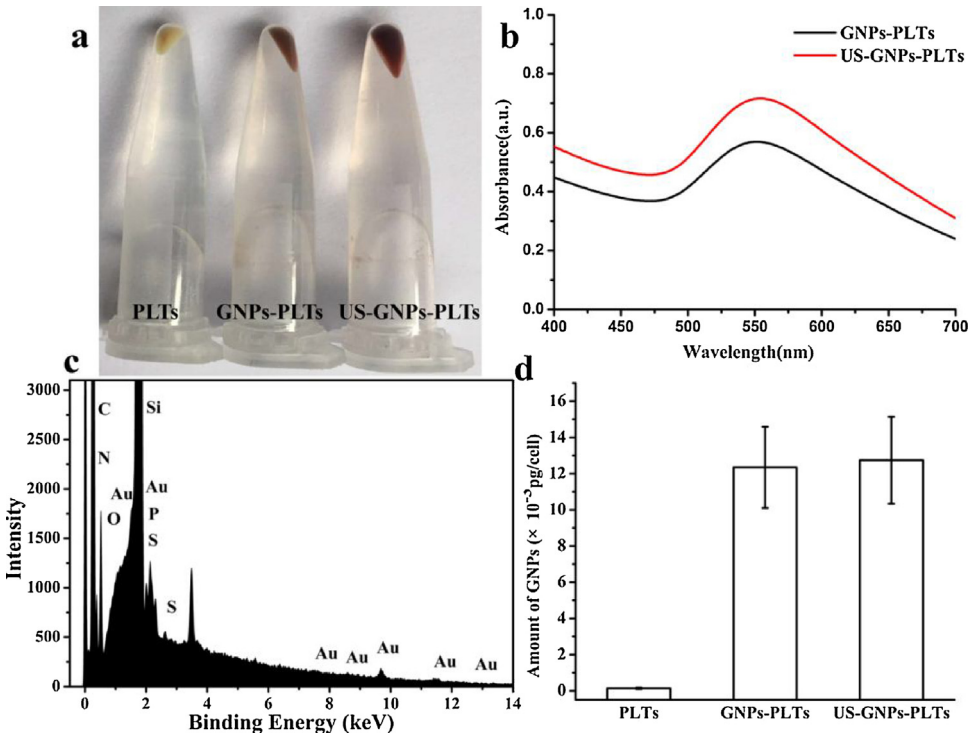

Fig. 1. Cell pellets photographs of platelets (a); UV–vis absorption spectra of GNPs-PLTs and US-GNPs-PLTs (b); X-ray energy-dispersive spectroscope of US-GNPs-PLTs (c); atomic absorption spectrometry results of PLTs, US-GNPs-PLTs and GNPs-PLTs, respectively (d).

by Coomassie Blue Staining Solution for 1.5 h (Beyotime Biotechnology, Haimen, China). The de-staining solution was prepared by ethanol (250 mL, 95%) and glacial acetic acid (80 mL) and the time of de-staining was approximately for 3 h.

2.7. SERS enhancement assay

Natural platelets and platelets after synthesis of GNPs were studied with SERS. The platelets suspension (0.1 mL) was placed onto a glass slide. SERS spectra were obtained using a Renishaw Invia Raman spectrometer, equipped with a Leica DMI300 B inverted microscope and a Peltier-cooled charge coupled device (CCD) detector. Power at the sample was 2–3 mW for a 1–2 μm laser spot size. Spectra were recorded between 1000 and 200 cm^{-1} at a resolution of 1–2 cm^{-1} and the laser exposure for each scan was ten seconds. The extracted data were further analyzed using Origin version 8.0.

2.8. Dark field imaging

Dark field optical imaging of platelets after synthesis of GNPs was studied by using an inverted microscope (Carl Zeiss, USA) with a digital camera. The platelets suspensions were placed onto a clean glass slide for imaging studies. Platelets were observed with a white light source with a high numerical aperture objective (NA 0.8, 40×). Then platelets were imaged in reflection mode which resulted from scattered light from GNPs in platelets.

2.9. CT imaging

Natural platelets and engineering platelets were washed 5 times with saline. Approximately 2.5×10^6 cells of each sample were resuspended and centrifuged at 3000 r/min for 5 min to obtain cell pellets. CT data were acquired using *In vivo* Micro-CT Hiscan-M1000 (Multimodality Molecular Imaging System for Small Animal, Southeast University). Imaging parameters were as follows: voltage, 80 kV; current, 0.5 mA. Reconstruction and volume rendered three-dimensional (3D) images were obtained using 3D Med 4.6 software.

2.10. Statistical analysis

Statistical analysis was conducted by at least three repeated experiments. A *p*-value less than 0.05 ($^*p < 0.05$, n = 3) was considered to be statistically significant.

3. Results

3.1. Synthesis of gold nanoparticles in platelets

Fig. 1a showed the cell pellets photographs of natural platelets (PLTs), platelets after GNPs synthesis (GNPs-PLTs) and platelets after GNPs synthesis with ultrasonic treatment (US-GNPs-PLTs) after centrifugation. Platelets were washed repeatedly to remove the GNPs in solution. It revealed that pellets turn from yellow to wine red after synthesis of GNPs, confirming that lots of GNPs were successfully synthesized in platelets, not only in solution.

To further verify the synthesis of intracellular GNPs, the engineered platelets were lysed and studied by UV–vis absorption spectrum. Fig. 1b showed the UV–vis absorption spectra of GNPs-PLTs and US-GNPs-PLTs. Both the engineered platelets with (US-GNPs-PLTs) and without ultrasound exposure (GNPs-PLTs) showed absorption at 550 nm, which was the characteristic absorption of Au nanoparticles. The results confirmed the synthesis of GNPs in platelets. Besides, absorption intensity of US-GNPs-PLTs was higher than that of GNPs-PLTs (0.72 and 0.57 for US-GNPs-PLTs and GNPs-PLTs respectively), implying the difference caused by ultrasound.

Fig. 1c showed the energy dispersive X-ray spectroscopy (EDS) of the engineered platelets. The elements of C, N, O, P and S could be easily distinguished, respectively, which originates from the cells. Atom Si in EDS pattern originated from the silicon slice for supporting SEM specimens. Au components could be found in both

US-GNPs-PLTs and GNPs-PLTs, but not exited in natural platelets (Fig. S1). The calculated atom contents of Au are 0.03% and 0.04% for GNPs-PLTs and US-GNPs-PLTs respectively (from a random region of 1 μm × 3 μm). The result of EDS further demonstrated the presence of Au in platelets.

Atomic absorption spectrometry (AAS) was used for the quantification of Au in platelets, which was shown in Fig. 1d. Synthesized Au content in each platelet was calculated by dividing the amount of Au measured with AAS by platelets counts. The amount of Au in GNPs-PLTs and US-GNPs-PLTs were $(12.3 \pm 2.2) \times 10^{-3}$ and $(12.7 \pm 2.4) \times 10^{-3}$ pg per one platelet respectively, while no Au existed in natural platelet. The large deviation may due to the complex biological microenvironment in living cell, which directly influences the *in situ* synthesis of Au content in intra-platelets. The amounts of Au synthesized in GNPs-PLTs and US-GNPs-PLTs showed no significant difference, which indicated that ultrasound exposure did not change the amount of GNPs synthesized in platelets.

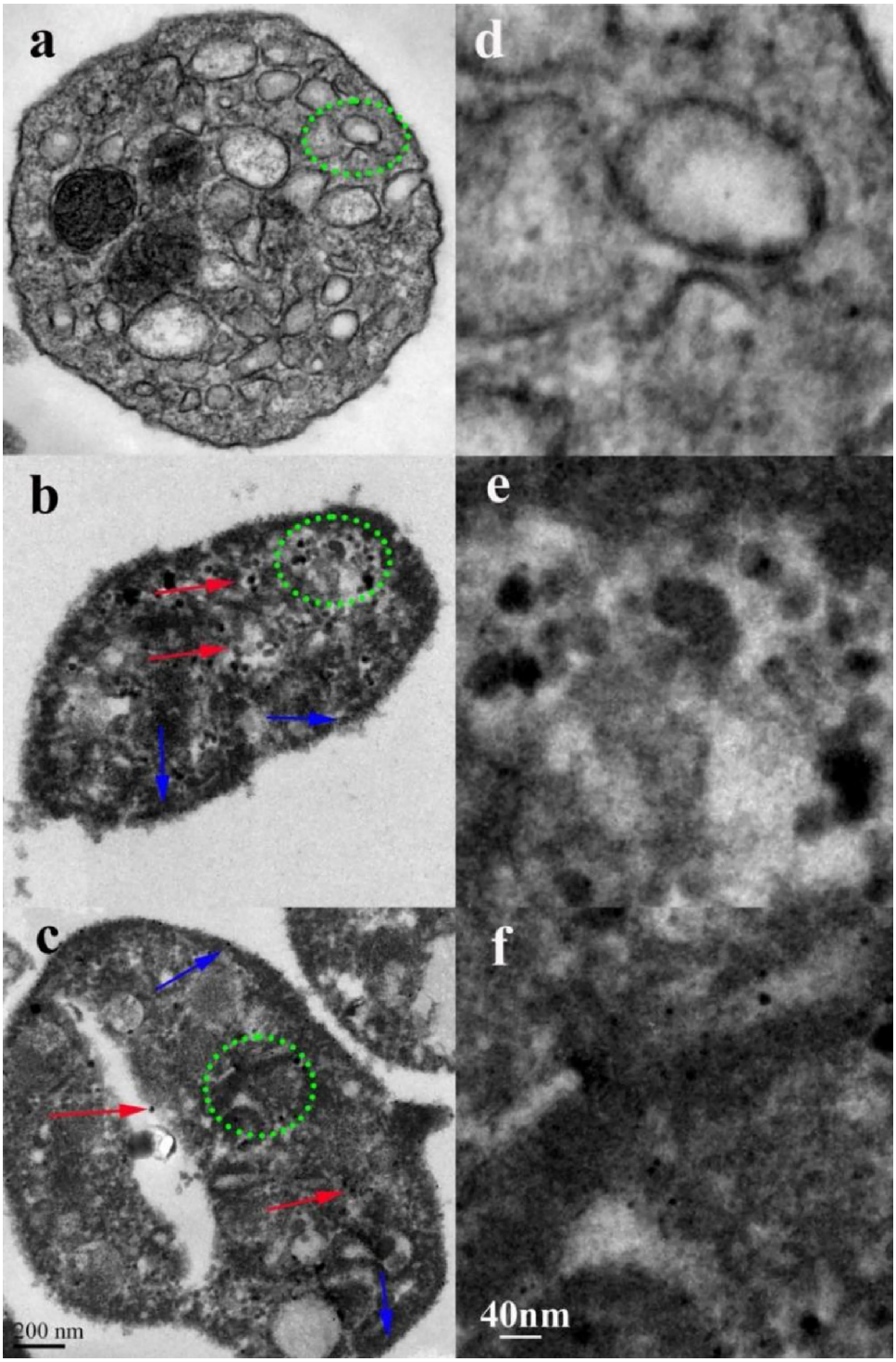

Fig. 2. TEM images of ultrathin section of PLTs (a), GNPs-PLTs (b) and US-GNPs-PLTs (c), and their 5 times magnifications of green circle respectively (d–f). (For interpretation of the references to colour in this figure legend, the reader is referred to the web version of this article.)

3.2. Intracellular distribution of gold nanoparticles in platelets

The intra-platelet GNPs distribution was further visualized by TEM, which was shown in Fig. 2. In Fig. 2a, natural platelets revealed well-developed tubular system with no cell nucleus. After GNPs synthesized *in situ*, platelets remained original shape and structure with no obvious finger-like projections extending from the cell, which indicates platelets were not activated (Fig. 2b and c). GNPs were successfully synthesized in the inner side of platelets. Many GNPs were located around the cell membrane (show as blue arrows). Besides, more particles were well dispersed in the cytoplasm of platelets (show as red arrows).

Fig. 2d–f showed the magnifications of local region in green circles. Specially, vesicles containing GNPs were not readily observed, indicating that particles didn't mainly enter cells *via* endocytosis. Many of GNPs were appeared near tubular system which is connected to the surface platelet membrane, implying that GNPs were synthesized from Au ions passing across cell membrane. As shown

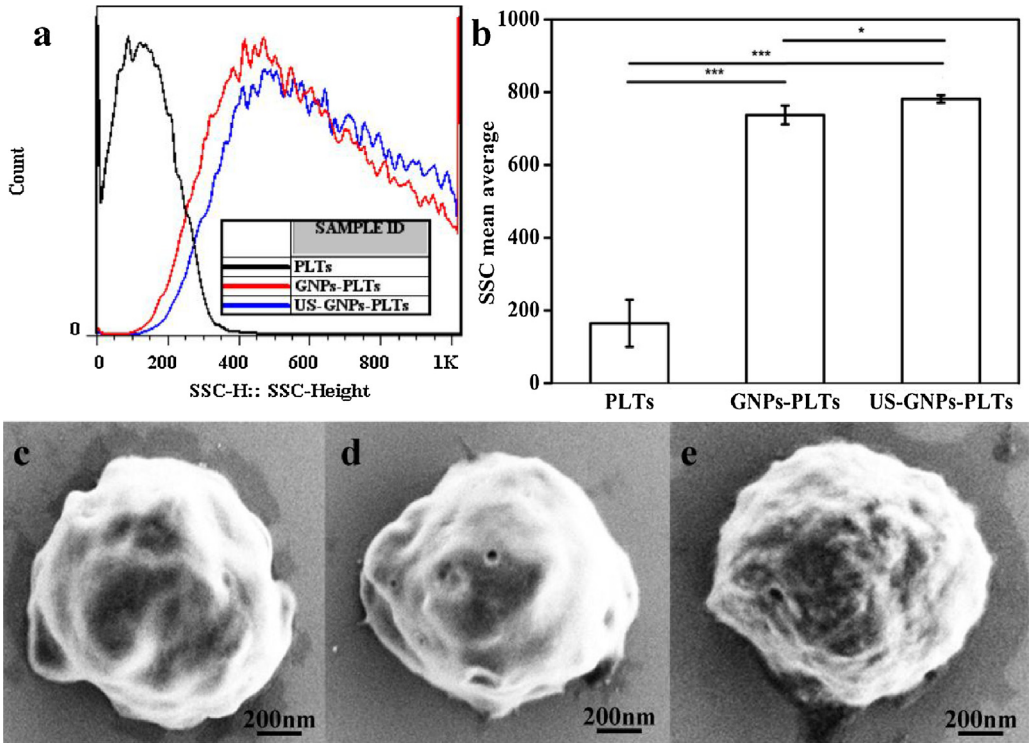

Fig. 3. Flow cytometric analysis of platelets analyzed by side scatting (a) and SSC mean average of PLTs, GNPs-PLTs and US-GNPs-PLTs(b). SEM images of PLTs (c), GNPs-PLTs (d) and US-GNPs-PLTs (e).

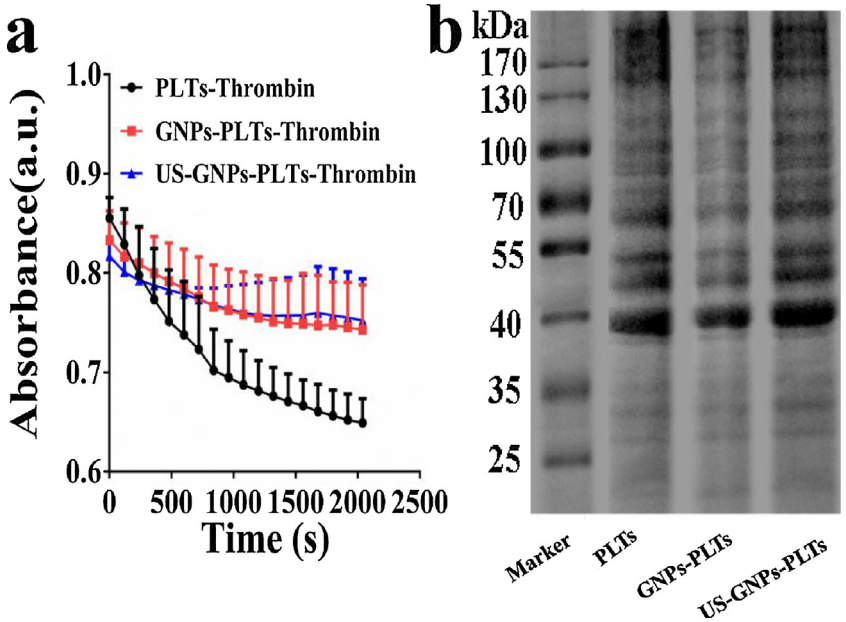

Fig. 4. Platelet aggregation assay. The PLTs, GNPs-PLTs and US-GNPs-PLTs were mixed with thrombin respectively followed by spectroscopic examination of solution turbidity (a). Protein bands results resolved using gel electrophoresis (b).

in Fig. 2c and f, with ultrasonic exposure during synthesis, the individual particle inside cells had a size of about 5 nm with very few aggregation, while most GNPs aggregate and have a bigger size of about 40 nm in cytoplasm in GNPs-PLTs group. Mono-dispersion of GNPs in cytoplasm indicates that ultrasound-assisted membrane permeability enhancement is beneficial for Au ion uniform distribution within the cell to prevent aggregation of synthesized nanoparticles.

3.3. Cellular GNPs loading analysis by SEM and flow cytometry measurement

The side scattering (SSC) measurement of platelets was used to further study the cellular loading of GNPs. The presence of nanoparticles can change cellular granularity, causing significant changes in the side light scattering. Fig. 3a showed the SSC results of PLTs, GNPs-PLTs and US-GNPs-PLTs, respectively. Nanoparticles were loaded in both GNPs-PLTs and US-GNPs-PLTs, as shown by the increase of side scatting compared with natural platelets. The peak value of side scatting shifts right in both GNPs-PLTs and US-GNPs-PLTs compared to natural PLTs. This result further indicates that GNPs were successfully loaded in platelets.

Fig. 3b showed the statistic SSC mean value of PLTs, GNPs-PLTs and US-GNPs-PLTs, respectively. The SSC value of GNPs-PLTs and US-GNPs-PLTs are significantly higher than PLTs. Besides, the peak of US-GNPs-PLTs has more horizontal displacement than GNPs-PLTs, and there is significant difference between GNPs-PLTs and US-GNPs-PLTs ($p < 0.05$). This phenomenon indicates that ultrasound exposure has a certainly impact on GNPs synthesis, which is consistent with the results of TEM.

Moreover, the SEM images were used to observe the surface change of platelets, which were shown in Fig. 3c–e. Platelets revealed biconvex discoid (lens-shaped) morphology and about 1 μm in diameter. After synthesis of GNPs, no obvious pseudopodia were found and platelets were not activated, which was agreement with TEM results. Surface of US-GNPs-PLTs was rougher than that of PLTs and GNPs-PLTs, implying that ultrasound exposure improves membrane permeability to synthesize GNPs in intra-platelets.

3.4. Influences of platelet after gold nanoparticles synthesis

Further, we investigated the influence of synthesis process on the platelets. The mean size of the PLTs and GNPs-PLTs were 1.7 ± 0.2 and 1.5 ± 0.4 μm, respectively. There was no significant difference. Zeta potential of GNPs-PLTs was -5.47 ± 0.28 mV, a bit higher compared with PLTs of -7.94 ± 0.76 mV. It is may be due to the presence of GNPs on cell membrane.

Aggregation performance is an important physiological characteristic of platelets, which is important for hemostasis and thrombosis process. Platelet aggregation has been the gold standard for evaluation of platelet function *in vitro* [36]. Fig. 4a showed the aggregation of PLTs, GNPs-PLTs and US-GNPs-PLTs mixed with thrombin, respectively. Addition of thrombin led to a decrease in absorbance over time in both GNPs-PLTs and US-GNPs-PLTs as natural platelets. It indicated that platelets maintained biological activity, and could be activated by thrombin. Both GNPs-PLTs and US-GNPs-PLTs exhibit the same aggregation tendency. The degree of platelets aggregation was lower in GNPs-PLTs and US-GNPs-PLTs compared to natural platelets, indicating the aggregation performance indeed can be affected by synthesis of GNPs. No significant difference between GNPs-PLTs and US-GNPs-PLTs reveals that ultrasound has little effect on platelet aggregation.

Platelets contain rich membrane protein content, including immunomodulatory proteins, CD47, CD59, and transmembrane proteins, GPIba, GPVI19, which is associated with platelets functions. Protein components were examined by gelelectrophoresis and shown in Fig. 4b. The protein bands of GNPs-PLTs and US-GNPs-PLTs are similar to natural platelets. Ultrasound-assisted rapid synthesis of GNPs *in situ* did not cause the change of protein composition and resulted in membrane protein retention.

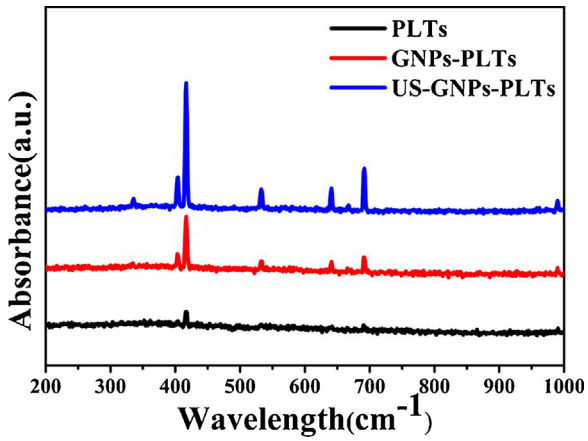

Fig. 5. SERS detection revealed surface enhanced Raman scattering in both GNPs-PLTs and US-GNPs-PLTs.

3.5. Surface-enhanced Raman spectroscopy

Gold nanoparticles can serve as substrates for surface-enhanced Raman scattering (SERS)-based detection because of their surface plasmon resonance (SPR)-induced optical and spectroscopic properties [37]. Raman spectrum of PLTs, GNPs-PLTs and US-GNPs-PLTs were shown in Fig. 5. Peak at 718 cm^{-1} was C—N vibration of polar head in phospholipids molecules [38]. Peak around 644 cm^{-1} was assigned to tyrosine from proteins. Peak at 417 cm^{-1} was attributed to vibration of Fe—O—O [38]. After GNPs were synthesized, characteristic peaks of platelet were enhanced as shown in spectrum of GNPs-PLTs and US-GNPs-PLTs. This result proved that the GNPs synthesized in platelets can be used as medium for surface-enhanced Raman scattering. Besides, peaks in US-GNPs-PLTs were enhanced more significantly than in GNPs-PLTs, suggesting that more effective cross sections were produced after ultrasound exposure.

3.6. Dark field imaging and CT imaging of platelets

The dark-field microscopy (DFM)-based imaging of GNPs in platelets was investigated. A population of platelets after synthesis of GNPs are shown in Fig. 6a–d, which were bright-field and dark-field images of GNPs-PLTs (Fig. 6a and b) and US-GNPs-PLTs (Fig. 6c and d) respectively. Platelets remain round without pseudopodia, and did not aggregate in Fig. 6a and b. Dark-field images highlights around platelets, which agreed well with the distribution of GNPs. The optical DFM results demonstrate GNPs can be rapidly synthesized in most of platelets. The scattering intensity of dark-field images was increased more significantly in US-GNPs-PLTs compared to GNPs-PLTs, which confirms the positive role of ultrasound in GNPs synthesis process. Thus, the fast synthesized GNPs can serve as useful probes for DFM-based imaging of platelets.

Gold nanoparticles possess favorable X-ray attenuating properties due to their high density and high atomic number [39]. CT imaging of platelets was carried out *in vitro*. Fig. 6e showed the CT images of cell pellets of PLTs, GNPs-PLTs and US-GNPs-PLTs respectively. White dots were significantly obvious in platelets pellets (show as red dotted line) and confirming that sufficient amount of GNPs synthesized in platelets. The CT signal intensity of GNPs-PLTs and US-GNPs-PLTs was 1.28 and 1.35 times of that PLTs (Table

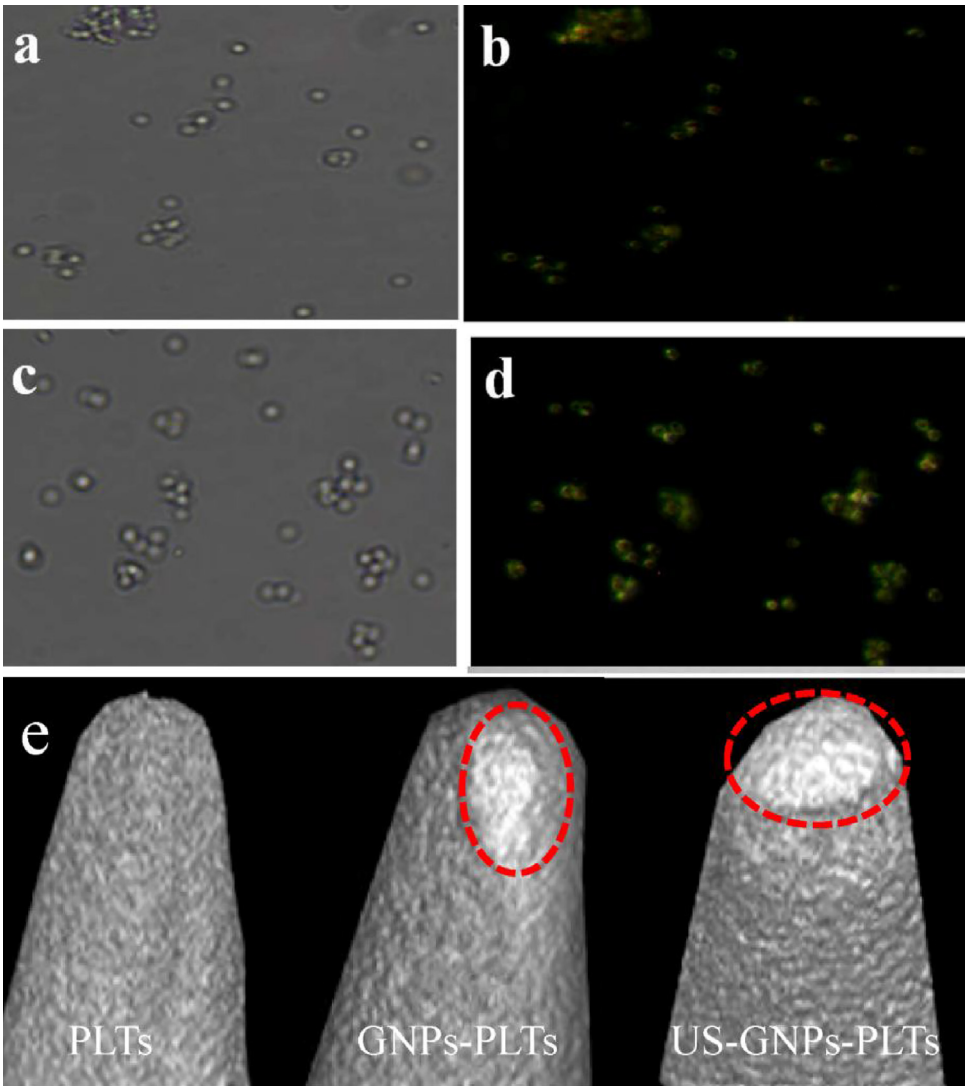

Fig. 6. Images of GNPs-PLTs and US-GNPs-PLTs under white light microscopy (a, b) and dark-field microscopy (c, d). The images of a–d were captured with the 40 times magnification. CT images of PLTs, GNPs-PLTs and US-GNPs-PLTs (e).

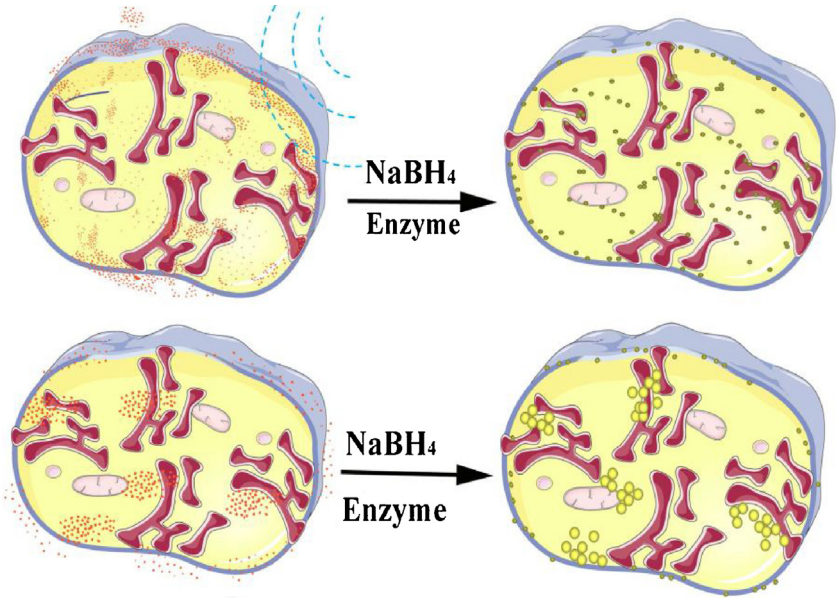

Fig. 7. Schematic diagram of ultrasound-assisted rapid *in situ* synthesis of gold nanoparticles in platelets.

S1), demonstrating the remarkable CT contrast signals provided by GNPs of platelets.

4. Discussion

We proposed a possible mechanism of ultrasound-assisted rapid *in situ* biosynthesihs of gold nanoparticles in living platelets as shown in Fig. 7. Rapid penetration across cell membrane, diffusion and sequestration in cytoplasm of $AuCl_4^-$ are thought as the first step of reaction. Investigations had reported that noble metal-centred anions could cross cell membranes and react as electron acceptors inside cells [40]. For platelets, one important factor is that it contains rich membranes derived from megakaryocytic smooth endoplasmic reticulum and they organized into a dense tubular system inside cell [41]. This dense tubular system is connected to the surface platelet membrane and thus it is greatly expanded the contact area of platelet and external environment. Then, the addition of $NaBH_4$ may initiate Au (0) seeds forming close to cell membranes and tubular system. It is clear from TEM images (Fig. 2) that the small or initial formation of GNPs occurs extremely close to cell membranes. Rapid and continuous synthesis of GNPs in cytoplasm may contain the activation of redox actors in enzymatic pools, resulting bigger size of GNPs in platelets cytoplasm. It reported that enzyme such as NAD(P)H-oxidases and NO-synthases [42,43] located in cytoplasm are effective actors in the reduction of Au (III) salts. During reaction, US exposure helps the sufficient amount of ions penetrating into the cytoplasm, resulting in small size and a better uniform distribution in the cytoplasm.

5. Conclusion

In conclusion, we have constructed a novel strategy of rapid and *in situ* synthesis of GNPs in living platelets. Due to rich membranes system in platelets, reactant ions can permeate easily into cells under ultrasound exposure. GNPs with size of about 5 nm were synthesized, which locates near tubular system including around membranes and in cytoplasm. Such mild reaction condition makes it possible for platelets to keep their natural hemostasis bioactivity. The biosynthesized GNPs in platelets can produce Raman enhancement effect and be probed by DFM-based imaging and CT imaging. Such mimicking GNPs-PLTs are expected to avoid recognition by the immune system in the future biomedical applications.

Conflict of interest

There are no conflicts to declare.

Acknowledgements

This investigation was financially funded by the project of National Natural Science Foundation of China (31370019, 61420106012), National Key Basic Research Program of China (2013CB733804) and National Key Research and Development Program of China (2017YFA0104302). And the funding partially also comes from the Fundamental Research Funds for the Central Universities (2242016K41072) and Zhong Ying Young Scholar of Southeast University. The authors also would like to thank the support from Collaborative Innovation Center of Suzhou Nano Science and Technology.

Appendix A. Supplementary data

Supplementary data associated with this article can be found, in the online version, at https://doi.org/10.1016/j.colsurfb.2018.01.009.

References

[1] J.V. Jokerst, S.S. Gambhir, Molecular imaging with theranostic nanoparticles, Acc. Chem. Res. 44 (2011) 1050–1060.
[2] K. Riehemann, S.W. Schneider, T.A. Luger, B. Godin, M. Ferrari, H. Fuchs, Nanomedicine-challenge and perspectives, Angew. Chem. Int. Ed. 48 (2009) 872–897.
[3] J.H. Ryu, S. Lee, S. Son, S.H. Kim, J.F. Leary, K. Choi, I.C. Kwon, Theranostic nanoparticles for future personalized medicine, J. Control. Release 190 (2014) 477–484.
[4] J. Di, J.C. Yu, Q. Wang, S.S. Yao, D.J. Suo, Y.Q. Ye, M. Pless, Y. Zhu, Y. Jing, Z. Gu, Ultrasound-triggered noninvasive regulation of blood glucose levels using microgels integrated with insulin nanocapsules, Nano Res. 10 (2017) 1393–1402.
[5] S. Su, H. Sun, W. Cao, J. Chao, H. Peng, X. Zuo, L. Yuwen, C. Fan, L. Wang, Dual-target electrochemical biosensing based on DNA structural switching on gold nanoparticle-decorated MoS2 nanosheets, ACS Appl. Mater. Interfaces 8 (2016) 6826–6833.
[6] D. Pissuwan, T. Niidome, M.B. Cortie, The forthcoming applications of gold nanoparticles in drug and gene delivery systems, J. Control. Release 149 (2011) 65–71.
[7] N. Manohar, F.J. Reynoso, P. Diagaradjane, S. Krishnan, S.H. Cho, Quantitative imaging of gold nanoparticle distribution in a tumor-bearing mouse using benchtop x-ray fluorescence computed tomography, Sci. Rep. 6 (22079) (2016), http://dx.doi.org/10.1038/srep22079.
[8] H.S. Peng, X.Y. Liu, G.T. Wang, M.H. Li, K.M. Bratlie, E. Cochrana, Q. Wang, Polymeric multifunctional nanomaterials for theranostics, J. Mater. Chem. B 3 (2015) 6856–6870.
[9] Y.-C. Yeh, B. Creran, V.M. Rotello, Gold nanoparticles: preparation, properties, and applications in bionanotechnology, Nanoscale 4 (2012) 1871–1880.
[10] T.K. Sau, C.J. Murphy, Room temperature, high-yield synthesis of multiple shapes of gold nanoparticles in aqueous solution, J. Am. Chem. Soc. 126 (2004) 8648–8649.
[11] X. Ji, X. Song, J. Li, Y. Bai, W. Yang, X. Peng, Size control of gold nanocrystals in citrate reduction: the third role of citrate, J. Am. Chem. Soc. 129 (2007) 13939–13948.
[12] J. Wang, G. Zhang, Q. Li, H. Jiang, C. Liu, C. Amatore, X. Wang, In vivo self-bio-imaging of tumors through *in situ* biosynthesized fluorescent gold nanoclusters, Sci. Rep. 3 (1157) (2013), http://dx.doi.org/10.1038/srep01157.
[13] D. Chen, C. Zhao, J. Ye, Q. Li, X. Liu, M. Su, H. Jiang, C. Amatore, M. Selke, X. Wang, *In situ* biosynthesis of fluorescent platinum nanoclusters: toward self-bioimaging-guided cancer theranostics, ACS Appl. Mater. Interfaces 7 (2015) 18163–18169.
[14] N.C. Sharma, S.V. Sahi, S. Nath, J.G. Parsons, J.L. Gardea-Torresdey, T. Pal, Synthesis of plant-mediated gold nanoparticles and catalytic role of biomatrix-embedded nanomaterials, Environ. Sci. Technol. 41 (2007) 5137–5142.
[15] M. Kitching, M. Ramani, E. Marsili, Fungal biosynthesis of gold nanoparticles: mechanism and scale up, Microb. Biotechnol. 8 (2015) 904–917.
[16] S. He, Z. Guo, Y. Zhang, S. Zhang, J. Wang, N. Gu, Biosynthesis of gold nanoparticles using the bacteria Rhodopseudomonas capsulata, Mater. Lett. 61 (2007) 3984–3987.
[17] P. Mukherjee, A. Ahmad, D. Mandal, S. Senapati, S.R. Sainkar, M.I. Khan, R. Ramani, R. Parischa, P. Ajayakumar, M. Alam, Bioreduction of $AuCl_4^-$ ions by the fungus, Verticillium sp. and surface trapping of the gold nanoparticles formed, Angew. Chem. Int. Ed. 40 (2001) 3585–3588.
[18] J. Wang, J. Ye, H. Jiang, S. Gao, W. Ge, Y. Chen, C. Liu, C. Amatore, X. Wang, Simultaneous and multisite tumor rapid-target bioimaging through *in vivo* biosynthesis of fluorescent gold nanoclusters, RSC Adv. 4 (2014) 37790–37795.
[19] D. MubarakAli, N. Thajuddin, K. Jeganathan, M. Gunasekaran, Plant extract mediated synthesis of silver and gold nanoparticles and its antibacterial activity against clinically isolated pathogens, Colloids Surf. B: Biointerfaces 85 (2011) 360–365.
[20] D. MubarakAli, J. Arunkumar, K.H. Nag, K.A. SheikSyedIshack, E. Baldev, D. Pandiaraj, N. Thajuddin, Gold nanoparticles from Pro and eukaryotic photosynthetic microorganisms-comparative studies on synthesis and its application on biolabelling, Colloids Surf. B: Biointerfaces 103 (2013) 166–173.
[21] M. Jeyaraj, R. Arun, G. Sathishkumar, D. MubarakAli, M. Rajesh, G. Sivanandhan, G. Kapildev, M. Manickavasagam, N. Thajuddin, A. Ganapathi, An evidence on G2/M arrest, DNA damage and caspase mediated apoptotic effect of biosynthesized gold nanoparticles on human cervical carcinoma cells (HeLa), Mater. Res. Bullet. 52 (2014) 15–24.
[22] Q. Wang, H. Cheng, H.S. Peng, H. Zhou, P.Y. Li, R. Langer, Non-genetic engineering of cells for drug delivery and cell-based therapy, Adv. Drug Deliv. Rev. 91 (2015) 125–140.
[23] H.S. Peng, C. Wang, X.Y. Xu, C.X. Yu, Q. Wang, An intestinal Trojan horse for gene delivery, Nanoscale 7 (2015) 4354–4360.
[24] G. Davì, C. Patrono, Platelet activation and atherothrombosis, New Engl. J. Med. 357 (2007) 2482–2494.
[25] J. Italiano, R. Shivdasani, Megakaryocytes and beyond: the birth of platelets, J. Thromb. Haemost. 1 (2003) 1174–1182.
[26] B. Nieswandt, S.P. Watson, Platelet-collagen interaction: is GPVI the central receptor? Blood 102 (2003) 449–461.

[27] D. Peters, M. Kastantin, V.R. Kotamraju, P.P. Karmali, K. Gujraty, M. Tirrell, E. Ruoslahti, Targeting atherosclerosis by using modular, multifunctional micelles, Proc. Natl. Acad. Sci. U. S. A. 106 (2009) 9815–9819.
[28] C.L. Modery-Pawlowski, L.L. Tian, V. Pan, K.R. McCrae, S. Mitragotri, A.S. Gupta, Approaches to synthetic platelet analogs, Biomaterials 34 (2013) 526–541.
[29] J.M. Chan, L. Zhang, R. Tong, D. Ghosh, W. Gao, G. Liao, K.P. Yuet, D. Gray, J.-W. Rhee, J. Cheng, Spatiotemporal controlled delivery of nanoparticles to injured vasculature, Proc. Natl. Acad. Sci. U. S. A. 107 (2010) 2213–2218.
[30] A.C. Anselmo, C.L. Modery-Pawlowski, S. Menegatti, S. Kumar, D.R. Vogus, L.L. Tian, M. Chen, T.M. Squires, A. Sen Gupta, S. Mitragotri, Platelet-like nanoparticles: mimicking shape, flexibility, and surface biology of platelets to target vascular injuries, ACS Nano 8 (2014) 11243–11253.
[31] C.M.J. Hu, R.H. Fang, K.C. Wang, B.T. Luk, S. Thamphiwatana, D. Dehaini, P. Nguyen, P. Angsantikul, C.H. Wen, A.V. Kroll, Nanoparticle biointerfacing by platelet membrane cloaking, Nature 526 (2015) 118–121.
[32] C.-M.J. Hu, R.H. Fang, B.T. Luk, K.N. Chen, C. Carpenter, W. Gao, K. Zhang, L. Zhang, 'Marker-of-self'functionalization of nanoscale particles through a top-down cellular membrane coating approach, Nanoscale 5 (2013) 2664–2668.
[33] T. Bai, Y. Tan, J. Zou, M. Nie, Z. Guo, X. Lu, N. Gu, $AuBr_2^-$-engaged galvanic replacement for citrate-capped Au-Ag alloy nanostructures and their solution-based surface-enhanced raman scattering activity, J. Phys. Chem. C 119 (2015) 28597–28604.
[34] D. Kim, Y.Y. Jeong, S. Jon, A drug-loaded aptamer-gold nanoparticle bioconjugate for combined CT imaging and therapy of prostate cancer, ACS Nano 4 (2010) 3689–3696.
[35] L. Fan, Y. Tian, R. Yin, D. Lou, X. Zhang, M. Wang, M. Ma, S. Luo, S. Li, N. Gu, Enzyme catalysis enhanced dark-field imaging as a novel immunohistochemical method, Nanoscale 8 (2016) 8553–8558.
[36] N. Moran, A. Kiernan, E. Dunne, R.J. Edwards, D. Shields, D. Kenny, Monitoring modulators of platelet aggregation in a microtiter plate assay, Anal. Biochem. 357 (2006) 77–84.
[37] T.K. Sau, A.L. Rogach, F. Jäckel, T.A. Klar, J. Feldmann, Properties and applications of colloidal nonspherical noble metal nanoparticles, Adv. Mater. 22 (2010) 1805–1825.
[38] W. Premasiri, J. Lee, L. Ziegler, Surface enhanced Raman scattering of whole human blood, blood plasma and red blood cells: cellular processes and bioanalytical sensing, J. Phys. Chem. B 116 (2012) 9376–9386.
[39] Q.Y. Cai, S.H. Kim, K.S. Choi, S.Y. Kim, S.J. Byun, K.W. Kim, S.H. Park, S.K. Juhng, K.H. Yoon, Colloidal gold nanoparticles as a blood-pool contrast agent for X-ray computed tomography in mice, Invest. Radiol. 42 (2007) 797–806.
[40] K. Tamaoki, N. Saito, T. Nomura, Y. Konishi, Microbial recovery of rhodium from dilute solutions by the metal ion-reducing bacterium Shewanella algae, Hydrometallurgy 139 (2013) 26–29.
[41] J.G. White, Interaction of membrane systems in blood platelets, Am. J. Pathol. 66 (1972) 295–312.
[42] M. Zayats, R. Baron, I. Popov, I. Willner, Biocatalytic growth of Au nanoparticles: from mechanistic aspects to biosensors design, Nano Lett. 5 (2005) 21–25.
[43] R.C. Jin, B. Voetsch, J. Loscalzo, Endogenous mechanisms of inhibition of platelet function, Microcirculation 12 (2005) 247–258.